JBC RESEARCH ARTICLE

The N-terminal domain of the *Agrobacterium tumefaciens* telomere resolvase, TelA, regulates its DNA cleavage and rejoining activities

Received for publication, January 28, 2022, and in revised form, April 8, 2022 Published, Papers in Press, April 18, 2022,
https://doi.org/10.1016/j.jbc.2022.101951

Siobhan L. McGrath, Shu Hui Huang, and Kerri Kobryn*

From the Department of Biochemistry, Microbiology & Immunology, College of Medicine, University of Saskatchewan, Saskatoon, Saskatchewan, Canada

Edited by Patrick Sung

Linear replicons can be found in a minority of prokaryotic organisms, including *Borrelia* species and *Agrobacterium tumefaciens*. The problem with replicating the lagging strand end of linear DNAs is circumvented in these organisms by the presence of covalently closed DNA hairpin telomeres at the DNA termini. Telomere resolvases are enzymes responsible for generating these hairpin telomeres from a dimeric replication intermediate through a two-step DNA cleavage and rejoining reaction referred to as telomere resolution. It was previously shown that the agrobacterial telomere resolvase, TelA, possesses ssDNA annealing activity in addition to telomere resolution activity. The annealing activity derives, chiefly, from the N-terminal domain. This domain is dispensable for telomere resolution. In this study, we used activity analyses of an N-terminal domain deletion mutant, domain add back experiments, and protein–protein interaction studies and we report that the N-terminal domain of TelA is involved in inhibitory interactions with the remainder of TelA that are relieved by the binding of divalent metal ions. We also found that the regulation of telomere resolution by the N-terminal domain of TelA extends to suppression of inappropriate enzymatic activity, including hairpin telomere fusion (reaction reversal) and recombination between replicated telomeres to form a Holliday junction.

Genome linearity is rare in the prokaryotic domain. A linear configuration of DNA requires a solution to a key problem presented by genome linearity: the end-replication problem. The end-replication problem refers to the difficulty of priming lagging strand synthesis at DNA termini without progressive loss of sequence from the ends (1, 2). Organisms from the genus *Borrelia*, *Agrobacterium tumefaciens* biovar I strains, and various phages have implemented the use of a covalently closed DNA hairpin turnarounds at the ends referred to as hairpin (hp) telomeres to circumvent this issue (3–8).

Hairpin telomeres are thought to solve the end-replication problem by eliminating the free ends. The prevailing model of replication of bacterial systems with hp telomeres is summarized in Figure 1*A*. An internal origin of replication serves as the initiation site for bidirectional replication that produces a replicated intermediate joined into a circular dimer at replicated telomere junctions (*rTels*). Thus, the end-replication problem has been solved, but the alternative problem of how to segregate the replicated intermediate to two daughter cells has arisen in its stead. This issue is solved by resolution of this replicated intermediate by a telomere resolvase that cleaves and rejoins the DNA at each *rTel* to regenerate linear daughters terminated by hp telomeres (5, 9, 10). This scheme posits the ability of the replisome to round the hp telomeres to complete replication. The production of the resulting replicated telomere junctions has been confirmed *in vivo* (11, 12).

The hp telomere resolvases, as an enzyme class, have been reviewed in the study by Kobryn and Chaconas (13). Biochemical and structural analyses of a handful of telomere resolvases have revealed the shared possession of a catalytic domain that cleaves and rejoins DNA using a domain structure and mechanism related to that of tyrosine recombinases and type IB topoisomerases (14–19). This mechanism requires no high-energy cofactors or divalent metal ions. Also revealed is an unexpected degree of domain diversity and evidence, at least *in vitro*, of multifunctionality (see Fig. 1*B* and (20–23)). Both the borrelial telomere resolvase, ResT, and the agrobacterial enzyme, TelA, possess a single-stranded DNA annealing activity. The annealing activities of ResT and TelA stem from their N-terminal domains as truncation of this domain [ResT (163–449) and TelA (107–442)]-eliminated annealing. Furthermore, the independently expressed N-terminal domains support annealing, albeit at a reduced efficiency compared to the full-length proteins (20, 21, 23). While the N-terminal domain of TelA is dispensable for telomere resolution, the longer deletion in ResT also abolished telomere resolution (23–27).

The ResT study in which the N-terminal domain and remaining two-thirds of the protein encompassing the catalytic and C-terminal domain were purified as independent proteins revealed that the larger ResT fragment responsible for *rTel* recognition and catalysis appears to guide binding of the N-terminal region containing the hp-binding module. Moreover, the N-terminal domain in the full-length protein appeared to mask the telomere recognition sites in the

* For correspondence: Kerri Kobryn, kerri.kobryn@usask.ca.

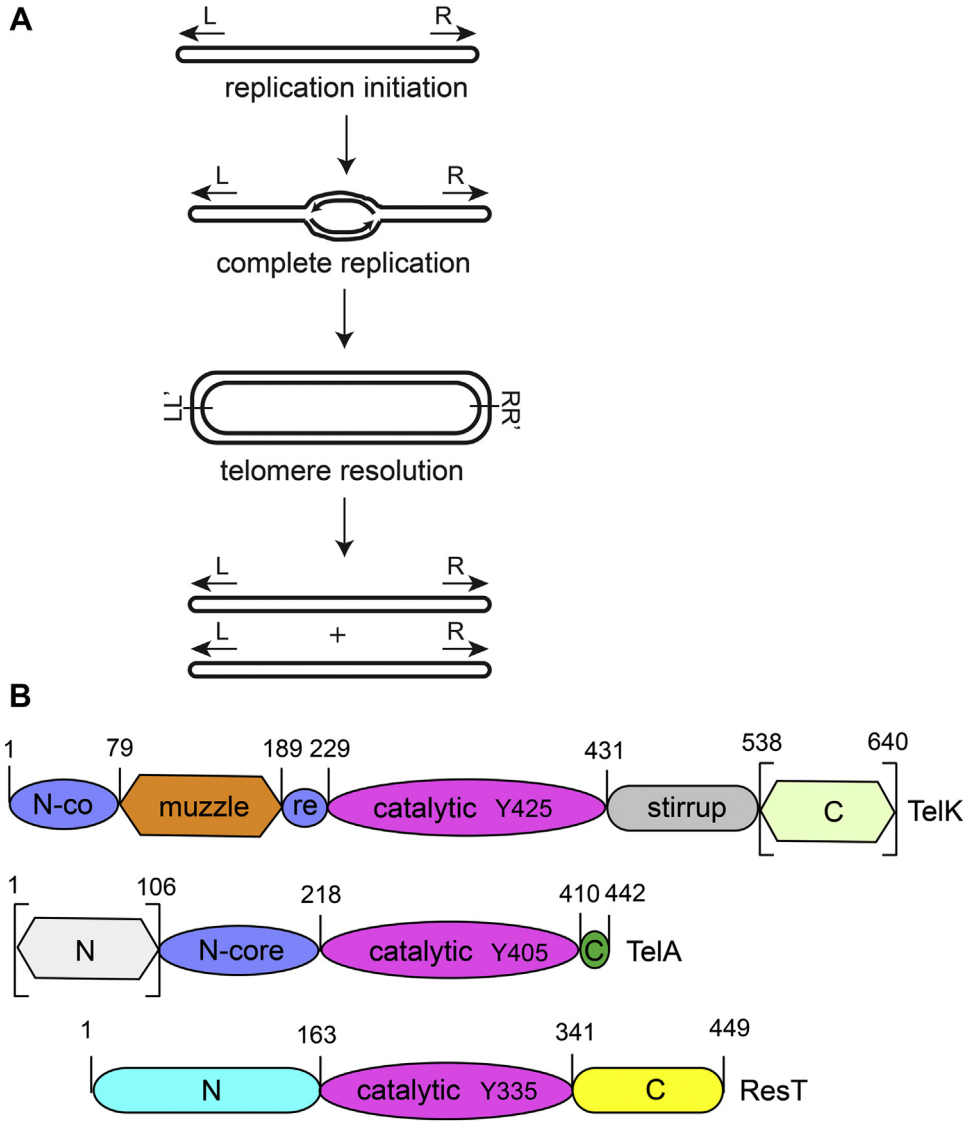

Figure 1. The Replication pathway of linear DNAs with hp telomeres and telomere resolvase domain organization. *A*, bidirectional replication of the chromosome initiates at an internal origin and continues until replication rounds the hairpin telomeres. A circular dimer intermediate results that is fused at replicated telomere junctions (denoted at L/L′ and R/R′). This intermediate is then resolved by a DNA cleavage and reunion reaction called telomere resolution that reconstitutes linear monomers terminated by hp telomeres. *B*, the domain architecture of three telomere resolvases characterized *in vitro*. TelK is the telomere resolvase from ΦKO2 of *Klebsiella oxytoca*, TelA is from *Agrobacterium tumefaciens*, and ResT is from *Borrelia burgdorferi*. Domains identified as homologous either through BLAST alignment or *via* structural analysis are identified in identically shaped and shaded domains (*i.e.*, N-core in TelK and TelA and the catalytic domain in all three resolvases). Domains without a homologous counterpart are given unique colors/shades. Domains that have been experimentally deleted without affecting telomere resolution are delimited in *square brackets*. The nucleophilic tyrosine is identified by amino acid number in the catalytic domains. hp, hairpin.

C-terminal region of ResT, suggesting that ResT is subject to autoinhibition by its N-terminal domain (25). This autoinhibition was capable of being overcome by positive supercoiling in the substrate DNA (28).

We report here that TelA is regulated by its dispensable N-terminal domain. By examining the properties of an N-terminal domain truncation mutant and of reactions with the N-terminal domain added back *in trans*, we found that telomere resolution by TelA is regulated by divalent metals and that much of this regulation is dependent upon the presence of the N-terminal domain. Furthermore, we also provide evidence that the N-terminal domain is involved in regulating the activity of the remainder of the enzyme by suppressing the competing reactions of hp telomere fusion and strand exchange between *rTels* (to produce Holliday junctions [HJs]).

Results

TelA is stimulated in the presence of a divalent metal ion

Telomere resolution by TelA has previously been demonstrated *in vitro* (19, 26). However, previous studies utilized micromolar concentrations of protein to promote telomere resolution, suggesting the use of less-than-ideal buffer conditions or the absence of an important accessory protein. Using a linearized plasmid containing a replicated telomere (*rTel*) junction, we observed its conversion into two hp products

when TelA was present in the reaction. Importantly, telomere resolution was greatly stimulated in the presence of a divalent metal ion with a preference for calcium over magnesium (Fig. 2, *B* and *D*). TelA was active over a larger range of magnesium (up to 8 mM) than with calcium, with greater than 4 mM of calcium becoming strongly inhibitory (Fig. S2). With divalent metal ion present, we only required low nanomolar concentrations of TelA for complete resolution. The presence of a divalent metal ion does not affect TelA affinity for its replicated telomere, suggesting the metal ion participates at a later step of telomere resolution than *rTel* recognition (Fig. S1).

We also examined the telomere resolution activity of the N-terminal truncation mutant of TelA, TelA (107–442). Removal of the N-terminal domain was previously shown to abolish the annealing activity *in vitro* (23). Therefore, we wanted to explore the effects of N-terminal domain deletion on telomere resolution as well. TelA (107–442) was found to be much more proficient at telomere resolution in the absence of divalent metal ions than wildtype TelA (Fig. 2, *C* and *E*). However, now the presence of excess divalent metal ion proved inhibitory with both magnesium and calcium suppressing resolution at concentrations above 6 and 2 mM, respectively (Fig. S2).

The fact that deletion of the N-terminal domain relieves TelA of the requirement for a divalent metal ion to promote efficient telomere resolution suggests that TelA may be subject to autoinhibitory regulation by its N-terminal domain. This regulatory mechanism can be relieved through removal of the autoinhibitory domain or by binding a divalent metal ion. The borrelial telomere resolvase, ResT, has also been shown to be subject to autoinhibition by its N-terminal domain (25).

Differential effects of mutating hp refolding residues in TelA

Our discovery of the important role played by divalent metal ions in TelA-promoted telomere resolution motivated us to revisit analyses made of key residues in TelA implicated in telomere resolution. Most information to date on the mechanistic details of TelA-promoted telomere resolution derives from a series of crystal structures made with a variety of substrates that captured different stages of the telomere resolution reaction pathway (19). One such structure used a substrate that prevented hp formation by using a half-site with a 5′-overhang missing a nucleotide; the resulting overhang lacked dyad symmetry and was too short to form an hp. The interactions captured in the resulting structure were hypothesized to represent a refolding intermediate of telomere

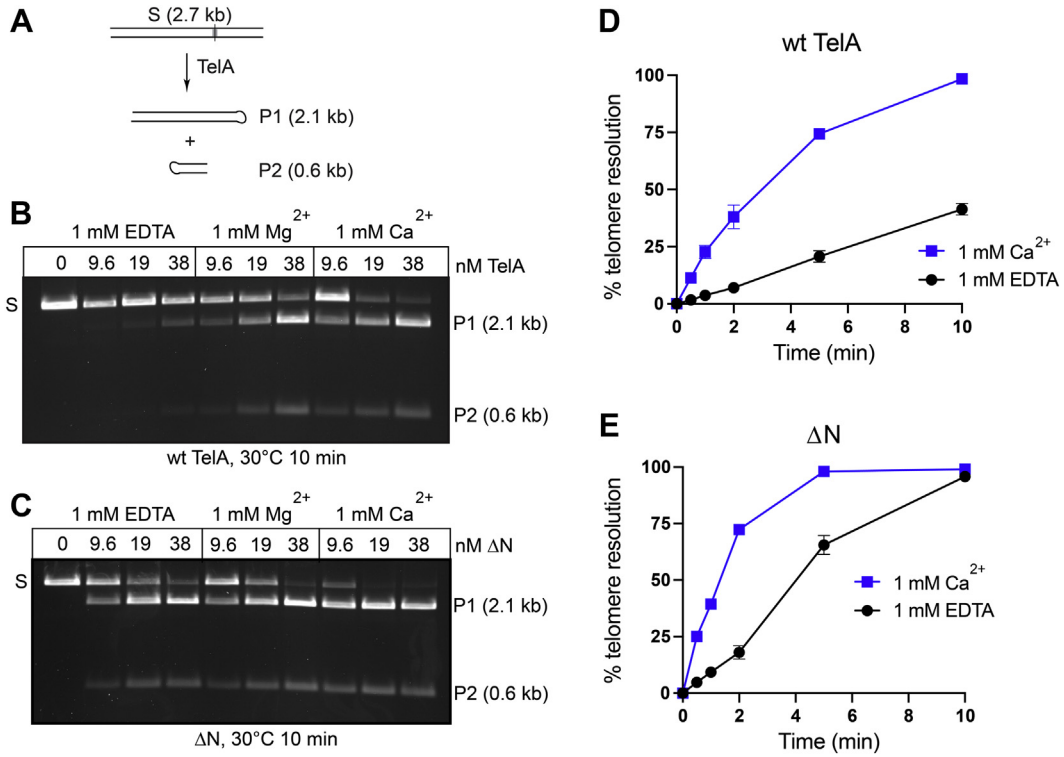

Figure 2. Deletion of the N-terminal domain reduces the divalent metal dependence of telomere resolution. *A*, schematic representation of the SspI-linearized plasmid substrate containing a 36-bp *rTel* junction (shaded and bisected by a *line*) and the resultant products of telomere resolution. The size (in kilobase pairs) is indicated for the plasmid substrate and the products of telomere resolution. S denotes the substrate, and P1 and P2 denote the telomere resolution products. *B*, 0.8% (w/v) agarose 1× TAE gel panel of telomere resolution reactions incubated at 30 °C for 10 min with the concentration of TelA indicated above the gel. The reaction buffer contained 1 mM EDTA, $MgCl_2$, or $CaCl_2$ as indicated in the loading key above the gel. *C*, 0.8% (w/v) agarose 1× TAE gel panel of telomere resolution reactions incubated at 30 °C for 30 min with the concentration of TelA (107–442) (ΔN) indicated above the gel. The reaction buffer contained 1 mM EDTA, $MgCl_2$, or $CaCl_2$ as indicated in the loading key above the gel. *D*, timecourse plots of telomere resolution reactions with 38 nM of wt TelA incubated with 1 mM EDTA or 1 mM $CaCl_2$. Reactions were performed in triplicate, and the mean and standard deviation are shown. *E*, timecourse plots of telomere resolution reactions with 38 nM of TelA (107–442) (ΔN) incubated with 1 mM EDTA or 1 mM $CaCl_2$. Reactions were performed in triplicate, and the mean and standard deviation are shown.

resolution (Fig. S3). In this structure, the refolding intermediate is stabilized by noncanonical base pairing across the refolding strands and by multiple interactions with TelA residues that interact with the extrahelical A6 base in the refolding strands. Included in these interactions are those made by the TelA D202 and R205 residues using both direct and water-mediated contacts. The researchers included an analysis of TelA (R205A) and determined the mutant to be cleavage competent, but unable to form hps (19). However, a mutant of the D202 residue was not included in the study. We constructed and purified TelA (D202A) and TelA (R205A) for further analysis of their phenotypes in conditions containing divalent metal ions. As these two residues appear to be involved at the same step of telomere resolution by stabilizing the extrahelical conformation of the A6 base in the cleaved and refolding strands, we hypothesized they would possess similar phenotypes.

While TelA (R205A) displayed the expected telomere resolution defect (Fig. S4), the D202A mutation unexpectedly hyperactivated telomere resolution and provided partial relief from the dependence on a divalent metal ion for efficient resolution (Figs. 3 and S4). Although TelA (D202A) could perform telomere resolution in the absence of a divalent metal ion, the presence of calcium or magnesium (4 mM) still mildly stimulated the reaction (Fig. 3*B*). Additionally, the addition of excess calcium or magnesium did not lead to reaction inhibition with the D202A mutant (Fig. S4). The hyperactive and semimetal-independent nature of TelA (D202A) indicates this residue may also be involved in autoinhibitory interactions regulating telomere resolution activity. Interestingly, telomere resolution by TelA (R205A) could be partially rescued when high concentrations of calcium were present but was unresponsive to the presence of magnesium (Fig. S4). Consistent with the original analysis of the R205A mutant, the resulting products were found to be primarily double-strand breaks rather than true hp telomere products. This, along with the eventual inhibition of telomere resolution in the presence of excess calcium but not magnesium for most TelA variants, suggests that there may be more than one metal-binding site in TelA.

The semimetal independence of TelA (D202A) prompted us to introduce this mutation into the N-terminal truncation mutant of TelA to test if the effects would be additive. The resulting double mutant [TelA (107–442; D202A)] produced a hyperactive and fully metal-independent phenotype in which addition of divalent metal ion did not lead to reaction stimulation. Similar to the case with the D202A mutation in isolation, the inhibitory effect of higher Ca^{2+} ion concentrations observed with wildtype TelA and the N-terminal truncation mutant was abolished in the double mutant (Figs. S4 and S5). Together, these results suggest that the both the D202 residue in the hp refolding module and the N-terminal domain are involved in interactions with the remainder of TelA to inhibit telomere resolution activity in the absence of divalent metal ions. Due to the additive effect of combining the D202A mutation with the N-terminal domain deletion, we speculate that D202 may activate TelA by interactions with a region of TelA distinct from the N-terminal domain.

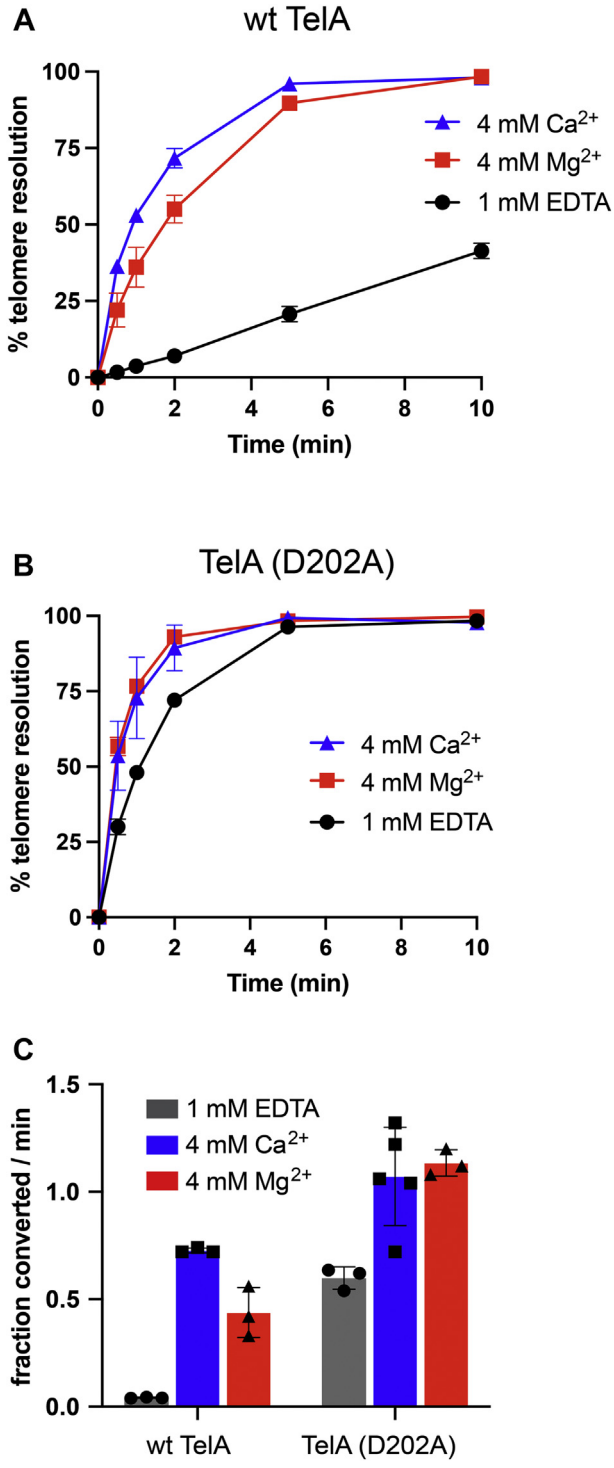

Figure 3. TelA (D202A) can perform telomere resolution independently of a divalent metal ion. *A*, telomere resolution timecourse plots with 38 nM wt TelA comparing 1 mM EDTA, 4 mM $MgCl_2$, and 4 mM $CaCl_2$ conditions. *B*, telomere resolution timecourse plots with 38 nM TelA (D202A) comparing 1 mM EDTA, 4 mM $MgCl_2$, and 4 mM $CaCl_2$ conditions. *C*, initial rates for 38 nM of wt TelA and TelA (D202A) for the divalent metal conditions are described in (*A*) and (*B*). All data plots show the mean and standard deviation of at least three independent experiments.

Addition of the TelA N-terminal domain in trans *to the truncation mutant restores autoinhibitory regulation*

Since deletion of the N-terminal domain seemed to relieve autoinhibition in TelA that normally rendered telomere

resolution responsive to the presence of divalent metal ions, we sought to determine if this metal responsiveness could be reinstated by addition of the N-terminal domain *in trans* to reactions performed by the truncation mutant. Adding increasing concentrations of TelA (1–106) *in trans* to both TelA (107–442) and TelA (107–442; D202A) re-established the phenotypes observed with the wildtype enzyme and TelA (D202A), respectively (Fig. 4*A*). When combined, the N-terminal truncation mutant and a 10-fold molar excess of the N-terminal domain displayed low levels of telomere resolution activity when a divalent metal ion was absent. As with the wildtype enzyme, reaction inhibition was relieved through the addition of calcium and, to a lesser extent, magnesium. Adding the N-terminal domain *in trans* with TelA (107–442; D202A) produced semimetal-independent telomere resolution where a divalent metal ion was not necessary but still stimulated the reaction (Fig. 4*B*). The reinstatement of autoinhibitory regulation by adding independent domains of TelA together suggested that these domains physically interact with one another.

Finally, in the presence of calcium, it was also noted that the addition of excess N-terminal domain *in trans* led to the production of a new reaction product designated as P3 (Fig. 4*B*). Reactions with the double mutant (ΔN; D202A) produced the greatest amount of this product. P3 seemed likely to be a fusion of P1 products since it had the appropriate gel mobility.

The N-terminal domain and TelA (107–442) physically interact

We tested the hypothesized interaction between the TelA N-terminal domain and TelA (107–442) and assessed the conditions in which it may occur, through protein–protein cross-linking studies (Fig. 5). Potential cross-linking of wildtype TelA, TelA (107–442), and TelA (1–106) to themselves was compared to a combination of the two proteins to separate self-interactions from interactions between the two individual protein fragments. In the presence of DNA and with buffer containing EDTA, wildtype TelA and TelA (107–442) were found to self-interact to some extent, producing cross-linking products upon treatment with dithiobis [succinimidylpropionate] (DSP) (Fig. 5; black arrows in the bracketing Western blot panels). Additionally, we observed that TelA (1–106) and TelA (107–442) interact with one another without a divalent metal ion present and in the presence of DNA (Fig. 5; red arrow in the bracketing Western blot panels). This interaction disappears when calcium is present in the reaction (Fig. 5; middle panels) or when DNA is omitted from the reaction (Fig. 5; right panels). To ensure that cross-linking of TelA (107–442) to itself was not due to contaminating nucleic acids in the protein preparation, we also conducted DSP cross-linking in the absence of added DNA and ensured that the protein preparations used were free of significant nucleic acid contamination (Fig. S6).

These data support the hypothesis that autoinhibition in TelA operates through protein–protein interactions between

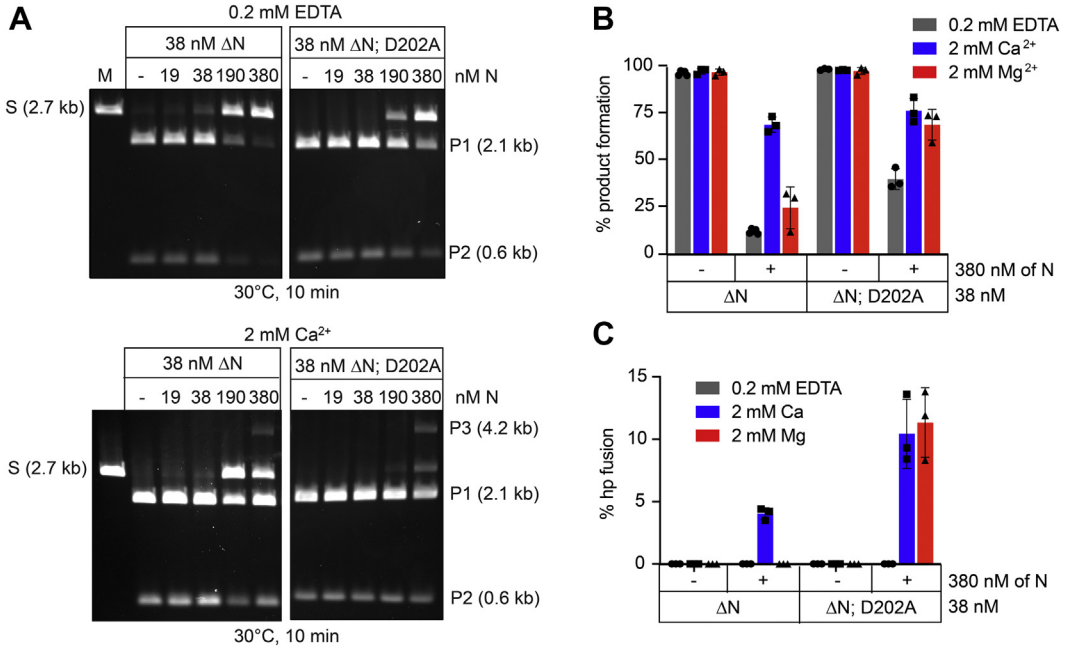

Figure 4. Titration of the N-terminal domain into reactions with TelA (107–442) and TelA (107–442; D202A). *A*, 0.8% (w/v) agarose 1× TAE gel panels of telomere resolution reactions incubated at 30 °C for 10 min with 38 nM TelA (107–442) or TelA (107–442; D202A) and a titration of TelA (1–106) added *in trans*. The reaction buffer contained either no divalent metal ions (0.2 mM EDTA) or 2 mM $CaCl_2$. M in the loading key above the gel indicates a protein-free reaction. S denotes the migration position of the substrate DNA, P1 and P2 denote the products, and P3 denotes the presumptive fusion product of the P1 hairpin telomeres. ΔN denotes TelA (107–442), ΔN; D202A denotes the double mutant, and N denotes TelA (1–106). *B*, % product formation (telomere resolution plus hairpin telomere fusion) plotted for telomere resolution reactions using 38 nM TelA (107–442) or TelA (107–442; D202A) on their own or in the presence of 380 nM TelA (1–106) added *in trans*. Conditions with 0.2 mM EDTA *versus* 2 mM $CaCl_2$ or $MgCl_2$ are shown. Reactions were performed in triplicate, and the mean and standard deviation are shown. *C*, % hp fusion abstracted from the reactions plotted in (*B*). Reactions were performed in triplicate, and the mean and standard deviation are shown. hp, hairpin.

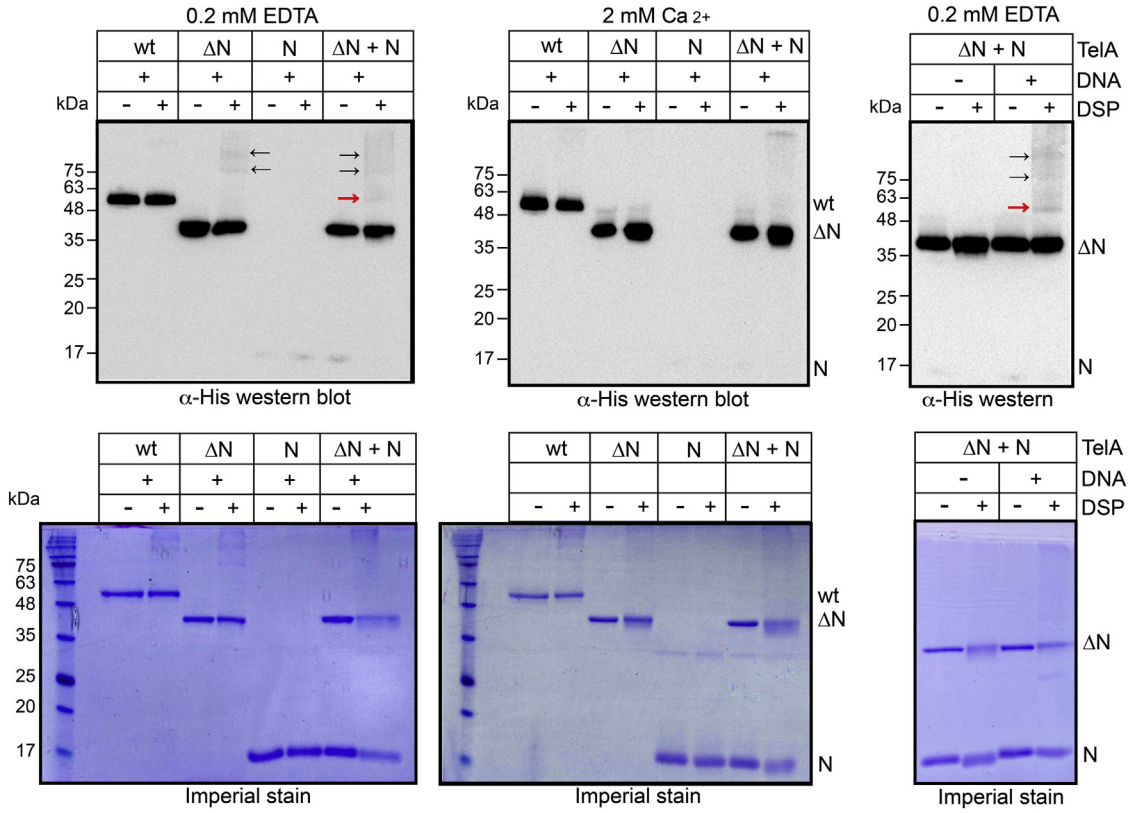

Figure 5. Chemical cross-linking of the interaction of the N-terminal domain with TelA (107–442). α-His Western blotting and Imperial Protein staining of 5%/10 to 18% (v/v) SDS-PAGE gradient gel panels for protein–protein cross-linking promoted by DSP (see Experimental procedures). wt denotes wildtype TelA, ΔN denotes TelA (107–442), and N represents TelA (1–106). Cross-linking of ΔN and N is indicated by the *red arrows*, and cross-linking of multiple ΔN to one another is indicated with *black arrows*. –/+ DNA denotes the presence or absence of 5 μg/ml SspI-digested pEKK392 in the reaction. wt and ΔN were present at 240 nM, and N was present a 1 μM. DSP, dithiobis [succinimidylpropionate].

the N-terminal domain and the rest of TelA. At least in the context of the N-terminal domain added *in trans*, the presence of DNA also appears important for this autoinhibitory interaction. Finally, calcium binding disrupts these interactions and removes the autoinhibition imposed on TelA by the N-terminal domain.

The N-terminal domain suppresses hp telomere fusion

The isoenergetic reaction chemistry of telomere resolvases, in principle, should render telomere resolution an intrinsically reversible reaction. Indeed, the borrelial resolvase, ResT, readily performs the reverse reaction by fusing hp telomeres at low reaction temperatures that disfavor the forward reaction or in extended reactions at standard temperatures (29). We observed full resolution with TelA when adequate concentrations of divalent metal ion were present and did not observe any products indicative of reaction reversal in standard reactions (Figs. 2, S2 and S4). Only under conditions where the N-terminal domain was added *in trans* to reactions with N-terminally truncated versions of TelA did we observe the formation of a potential reversal product (P3). The P3 product had a migration mobility (4.2 kb) consistent with it being a fusion product of two P1 hps (Fig. 4*A*; bottom panel). On occasion we were also able to see a product of the expected size if two P2 hp's had been fused (Unpublished results). This discrepancy is probably due to easier detection by ethidium bromide staining of the longer P3 product (4.2 kb *versus* 1.2 kb). Therefore, we tested if TelA had the ability to fuse hp telomeres by monitoring the conversion of oligonucleotide hp telomere substrates into an *rTel* product with our handful of TelA mutants used under a variety of reaction conditions. To test the conditions for the effect on TelA activity, we also conducted reactions with a control substrate that lacked the hp turnaround. This control is a half-site that when cleaved by TelA becomes a suicide substrate that traps TelA on the cleaved DNA (Fig. 6*A*; schematic). Under temperatures optimal for telomere resolution (30 °C), the wildtype enzyme and all mutants displayed cleavage competency with the exception of the N-terminal domain on its own (Fig. 6*A*; left panel). However, none of TelA variants promoted hp fusion (Fig. 6*B*; left panel). At low reaction temperatures that block telomere resolution (5 °C), wildtype TelA and the D202A mutant but not the truncation mutants were found to be cleavage competent (Fig. 6*A*; middle panel). None showed any evidence of supporting hp telomere fusion. However, addition of the N-terminal domain *in trans* with either TelA (107–442) or TelA (107–442; D202A) stimulated both half-site DNA cleavage and hp fusion at 5 °C (Fig. 6, *A* and *B*; middle panels). Both hp fusion and half-site cleavage required the conservation of the *rTel* sequence for activity since reactions with control mock telomeric half-sites or mock hp telomeres yielded no

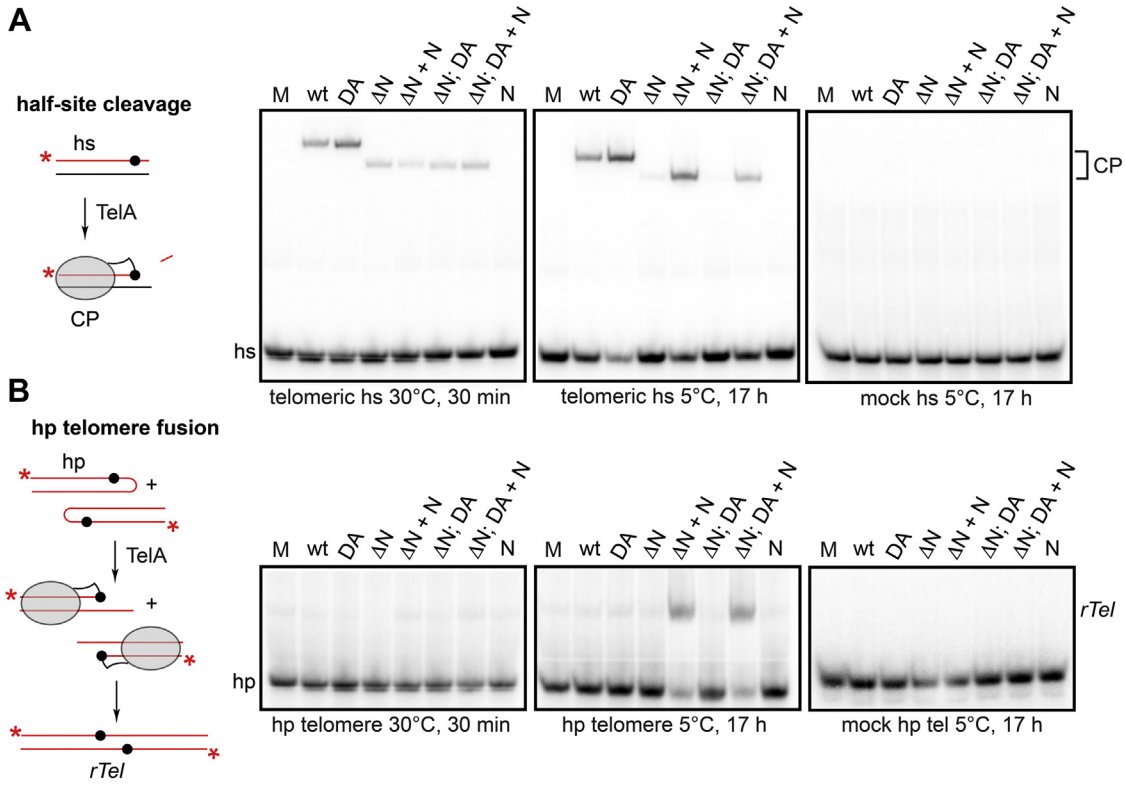

Figure 6. Fusion of oligonucleotide hp telomeres. *A*, cleavage of a half-site substrate comprised the sequence present in the hp telomeres but without the presence of the hp turnaround. Cleavage of the half-site is followed by diffusion away of the three nucleotides distal to the scissile phosphate trapping TelA on the cleaved half-site. This migrates in the "cleavage product" (CP) position of the gel. The N-terminal deletion mutants of TelA produce a faster migrating CP due to the missing mass of the deleted N-terminal domain. The mock versions of these substrates were produced by changing all T's to A's, A's to T's, G's to C's, and C's to G's. This maintains the sequence composition of the half-site and hp telomere substrates but produces a scrambled version that should not be recognized by TelA. wt denotes wildtype TelA (wt), and DA and ΔN denote TelA (D202A) and TelA (107–442), respectively, and their combination within a double mutant (ΔN; DA). When the TelA (1–106), the N-terminal domain is added *in trans*, this is indicated in the gel loading keys by +N. Shown are 8% (v/v) PAGE 1× TAE/0.1% (w/v) SDS gels of reactions performed with 5′-end-labeled substrate. *B*, fusion of hp telomeres by reversal of the telomere resolution reaction produces a replicated telomere (*rTel*) as the product. The details of the gel loading key are as noted for (*A*). Shown are 8% (v/v) PAGE 1× TAE/0.1% (w/v) SDS gels of reactions performed with 5′-end-labeled substrate. All reactions contain 76 nM TelA and 2 mM $CaCl_2$. The incubation temperatures and duration are noted below the gels.

products (Fig. 6, *A* and *B*, right panels). Under these conditions, a significant preference for calcium over magnesium or EDTA (Fig. S7) was observed with only the ΔN; D202A double mutant, supporting significant hp telomere fusion with magnesium (Fig. S7).

Only under the highly artificial reaction conditions used here where (1) the N-terminal domain is added back *in trans* at a 10-fold molar excess to a truncation mutant of that domain and (2) where the reactions are incubated at a low temperature (5 °C) that inhibits the forward reaction do we observe the accumulation of hp telomere fusion products. Because of the autoinhibition imposed by the N-terminal domain on telomere resolution in the absence of divalent metal ions, it is tempting to conclude that the N-terminal domain also plays a role in inhibiting hp telomere fusion in the context of the full-length enzyme. In this view, the N-terminal truncation mutants are able to promote hp telomere fusion, but the forward reaction causes the immediate resolution of the fused *rTel* back into hp telomeres at 30 °C, obscuring this activity. At 5 °C, the situation is more complex in that the cleavage reaction with the truncation mutants seems to require addition of the N-terminal domain *in trans*. Here, once cleavage chemistry has occurred, hp telomere fusion can occur and the *rTel* accumulates due to a lack of the competing forward reaction. It is unknown, in this artificial context, why DNA cleavage by the N-terminal truncation mutants seems to need participation of the N-terminal domain added *in trans*. It is also formally possible that the N-terminal domain added *in trans* maybe play a role in hp telomere fusion beyond stimulating DNA cleavage by the truncation mutants at 5 °C.

The N-terminal domain suppresses recombination between replicated telomere junctions

Under conditions unfavorable for telomere resolution including low temperatures and the presence of negative supercoiling in the DNA substrates, ResT possesses the ability to catalyze strand exchange between replicated telomeres (*rTels*) to form an HJ—an intermediate found in site-specific recombination reactions promoted by the related tyrosine recombinases (30). We wanted to examine whether TelA could perform this side reaction as well. The ability to form HJs was analyzed by incubating the negatively supercoiled *rTel*-containing plasmid, pEKK392, with a radiolabelled

oligonucleotide *rTel* substrate with or without the enzyme. The oligonucleotide *rTel* possesses heterologous sequences on both flanks to prevent branch migration after HJ formation (Table S1). Successful strand exchange would result in the plasmid substrate remaining negatively supercoiled but becoming radiolabelled (Fig. 7*A*). This can subsequently be visualized through a combination of autoradiography and ethidium bromide staining of agarose gels. We found that HJ formation occurred in reactions containing N-terminal truncations of TelA (and Ca^{2+}) whether or not the N-terminal domain had been added to the reaction *in trans* (Fig. 7*B*; left panel). As a control we determined that HJ formation was only observed when the *rTel* sequence was conserved; reactions with a mock *rTel* yielded no products (Fig. 7*B*; right panel). To confirm the identity and position in the plasmid of the HJ, we further analyzed reactions performed with TelA (107–442; D202A) as they produced the greatest amount of HJ. Aliquots of HJ formation reactions were further processed by AhdI digestion, by treatment with the HJ resolvase T7 endonuclease I or by AhdI linearization followed by T7 endonuclease I treatment (Fig. 7*A*). The results in Figure 7*C* show that the negatively supercoiled pEKK392 plasmid in protein-free reactions was partially converted into linear product, indicating that the 35-bp inverted repeat represented by the *rTel* was sometimes extruded into a cruciform that could be resolved by T7 endonuclease I. The majority of the radiolabelled HJ formed by the TelA double mutant was resolved by T7 endonuclease I treatment. When the HJ was processed by linearization with AhdI followed by resolution with T7 endonuclease I, the HJ was resolved into two radiolabelled products of the size expected if HJ formation occurred between the oligonucleotide *rTel* and the *rTel* cloned into the plasmid at the BamHI site in the plasmid multiple cloning site (Fig. 7, *A* and *C*). The analysis in Fig. S8 revealed that recombination between *rTels* to form HJs promoted by the ΔN mutant was favored by Ca^{2+} over Mg^{2+} but that the ΔN; D202A mutant could support some recombination in EDTA and showed recombination levels in Mg^{2+} similar to those seen in Ca^{2+}. Since deletion of the N-terminal domain allowed recombination between two *rTel*s, we sought to determine if addition of N *in trans* would inhibit recombination. Fig. S9 shows that addition of a 5- to 20-fold molar excess of N added *in trans* reduces the yield of HJ with the ΔN mutant but not with the hyperactivated ΔN; D202A double mutant.

Once again, TelA could only perform the competing side reaction of recombination between *rTel*s when the N-terminal domain was absent. This further highlights the importance of the N-terminal domain in regulating telomere resolution and suppressing potential competing reactions.

Discussion

The role of divalent metal ions in regulation of TelA activity

Initial reports of TelA utilized micromolar concentrations of protein in order to obtain full resolution (19, 26). We report here that telomere resolution promoted by TelA is significantly stimulated by divalent metal ions allowing low nanomolar concentrations of enzyme to be used to achieve complete reactions. Calcium ions are preferred over magnesium ions but actually become inhibitory if present in concentration above 2 to 4 mM (Figs. 2 and S2). Divalent metal ions are not required for catalysis of telomere resolution (14, 15, 18, 19). However, there is precedent for a stimulatory role for calcium with a phage-encoded telomere resolvase (TelN) (14).

Deletion of the N-terminal domain allows TelA to become active without addition of divalent metal ions, though addition of excess calcium still inhibits telomere resolution promoted by the ΔN mutant (Figs. 2 and S2). Mutation of D202 to alanine similarly activates TelA to become partially metal-independent and relieves the inhibition seen with excess calcium ion addition (Figs. 3 and S4). Combining the N-terminal domain deletion with the D202A mutation produces a TelA that is hyperactivated, metal-independent, and insensitive with respect to telomere resolution (Figs. 4 and S5).

We infer from this pattern of reactivity that TelA possesses at least two divalent metal ion–binding sites, one in the N-terminal domain and a second site somewhere in the remainder of the protein that binds divalent metal ions with lower affinity. When this second site is filled by calcium, telomere resolution is inhibited rather than stimulated. This second site is disrupted, either directly or indirectly, by the D202A mutation.

When the N-terminal domain is added *in trans* to reactions with the ΔN mutant, this re-establishes the metal dependence of telomere resolution. We infer from this that binding of divalent metal ions relieves an autoinhibitory interaction between the N-terminal domain and the remainder of the protein (Fig. 4). This interpretation is supported by the detection, *via* protein–protein cross-linking studies, of interactions between ΔN and the N-terminal domain added *in trans*. This interaction is disrupted by addition of divalent metal ions (Fig. 5). These interpretations are summarized in our model presented in Figure 8.

The *Borrelia burgdorferi* telomere resolvase, ResT, has been reported to be subject to autoinhibition, with the full-length enzyme showing very poor affinity for *rTel*s unless positive supercoiling is present in the substrate DNA or the ResT N-terminal domain is deleted (25, 28). The ResT N-terminal domain deletion mutant is, however, defective for telomere resolution so does not represent a separation of function mutant like the ΔN mutant of TelA does (23, 25). Autoinhibition in ResT is operative at the level of substrate binding but must occur at a different reaction stage in TelA since divalent metal ions have no impact on affinity for an *rTel* substrate (Fig. S1). Possessing enzymes that cleave and/or rearrange DNA is risky business for cells; therefore, there is strong selection for tight regulation of such activities. Among the regulatory mechanisms used is autoinhibition. Examples include the bacterial Mre11/Rad50 exonuclease and endonuclease complex that is held in an autoinhibited conformation until a DNA end is recognized resulting in repositioning of the Mre11 subunits relative to Rad50 subunits (31), the autoinhibitory domain of RAG2 that renders V(D)J recombination

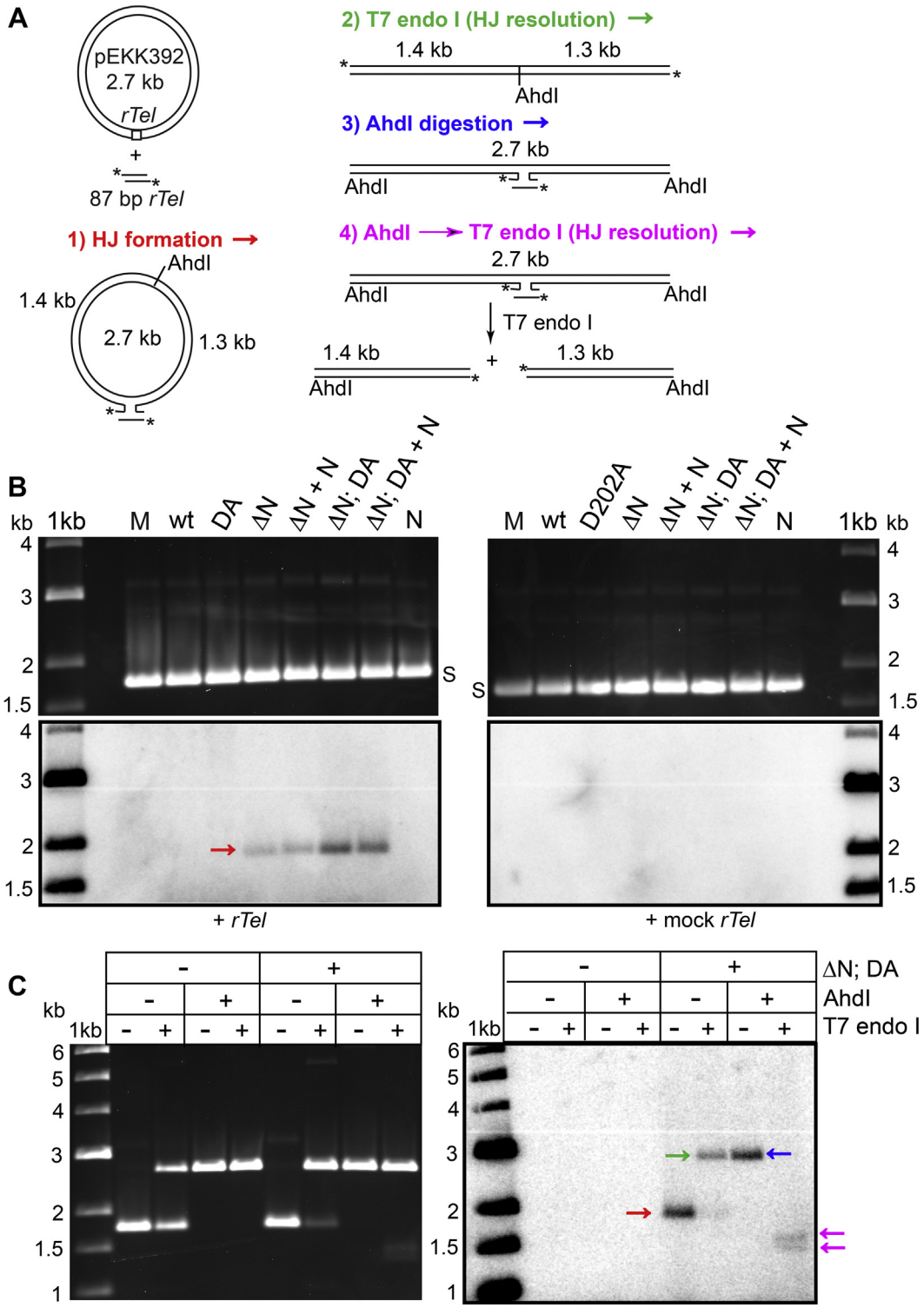

Figure 7. Recombination between replicated telomeres. *A*, schematic representation of a strand exchange reaction between negatively supercoiled pEKK392 and a 5′-^{32}P end-labeled (*) 87-bp oligonucleotide *rTel*. HJs resulting from this strand exchange can be resolved with T7 endonuclease I. Linearization with AhdI prior to T7 endonuclease I treatment results in resolution into two products due to the opposing strand scission sites of the two enzymes. The cleavage position of AhdI is labeled in the diagram. *B*, autoradiogram and ethidium bromide–stained 0.8% (w/v) agarose 1× TAE gel panels of HJ formation between 10 μg/ml pEKK392 and 70 nM of either end-labeled *rTel* (OGCB827*/828*) or mock *rTel* (855*/856*) in 2 mM Ca^{2+}. wt denotes wildtype TelA, and DA and ΔN denote TelA (D202A) and TelA (107–442), respectively, and their combination within a double mutant (ΔN; DA). TelA (1–106) is denoted by N, and when added *in trans*, by +N. All proteins were present at 76 nM besides N which was present at 380 nM. *C*, autoradiogram and ethidium bromide–stained 0.8% (w/v) agarose 1× TAE gel panel of HJ formation between 10 μg/ml pEKK392 and 65 nM end-labeled *rTel* with or without 76 nM of the double mutant (ΔN; DA). AhdI and/or T7 endo I treatment was applied as indicated in the panel legend. HJ, Holliday junction.

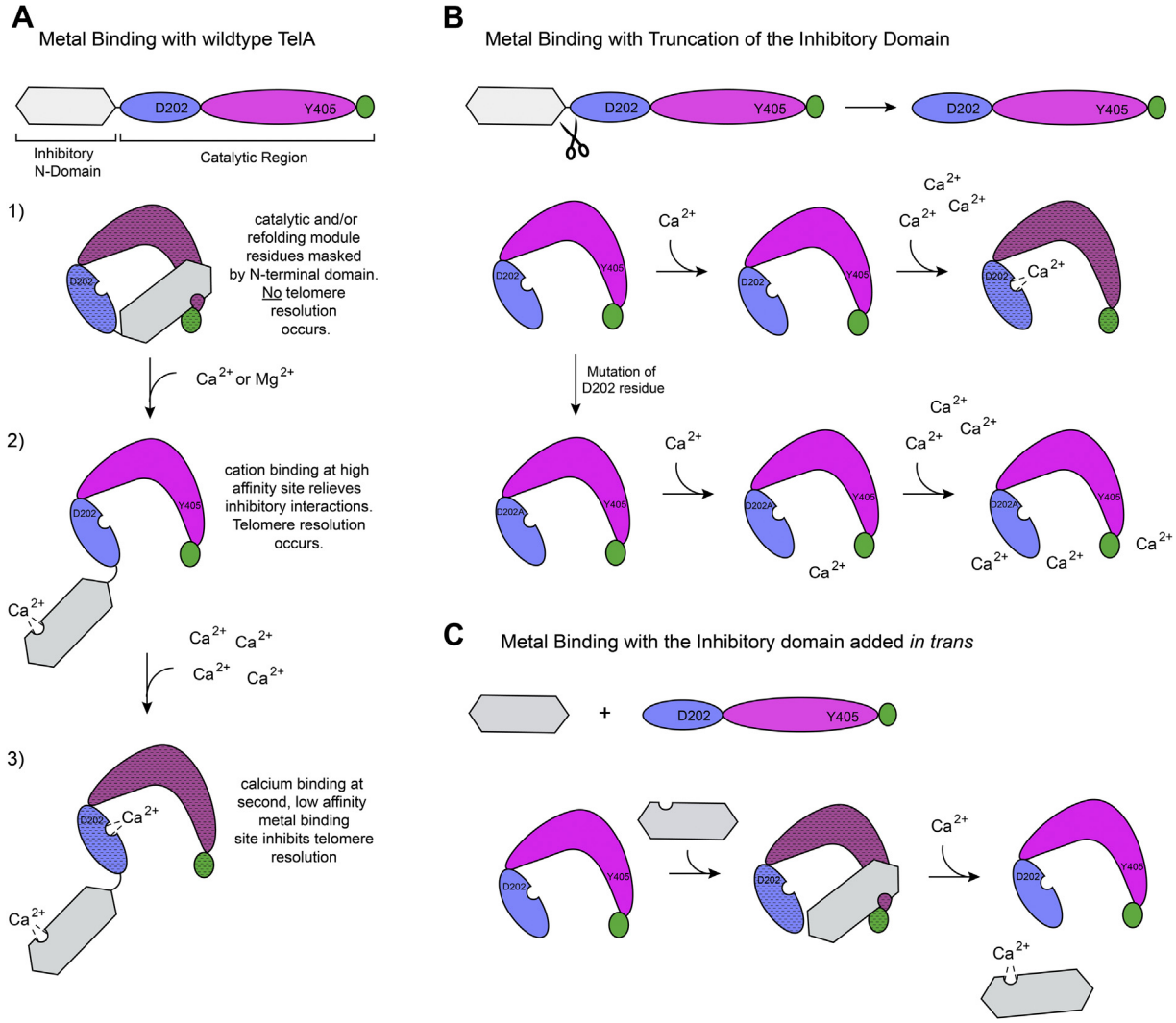

Figure 8. Model of TelA regulation. Models for metal binding with wildtype TelA (*A*), N-terminal truncation mutant of TelA (*B*), and the N-terminal domain being added *in trans* (*C*) are shown. *A*, the N-terminal domain of TelA physically interacts with the remainder of TelA, masking the catalytic and/or refolding module residues and rendering the enzyme inactive (represented by the stippled shading of the domains). The presence of low levels of a divalent metal ion (with a preference for calcium) results in metal binding to a high-affinity site in the inhibitory N-terminal domain. This relieves the inhibitory effect of the N-terminal domain, and the enzyme is in its active conformation. High calcium concentrations stimulate binding at a second, low-affinity metal-binding site located in proximity to the D202 residue. Ca^{2+} binding at this second site inhibits enzymatic activity. *B*, truncation of the inhibitory N-terminal domain removes the high-affinity metal-binding site and leaves the enzyme in its open, active conformation. Addition of low calcium concentrations has no effect on the truncation mutant of TelA. High calcium concentrations still lead to binding at the low-affinity metal-binding site and render the enzyme inactive. Mutation of the D202 residue disrupts binding at the low-affinity metal-binding site, resulting in high calcium concentrations having no effect on enzymatic activity. *C*, addition of the N-terminal domain *in trans* with the rest of TelA re-establishes the inhibitory protein–protein interactions observed with the wildtype enzyme. Exposure to low calcium concentrations results in metal binding at the high-affinity site and disruption of the inhibitory interactions.

responsive to active chromatin marks (32), and the stacking of the C-terminal helix of the Cre recombinase, *in cis*, over the enzyme active site until *loxP* binding and synapsis rearranges this helix into a *trans* stimulatory role (33).

The role of the N-terminal domain in regulation of TelA activity

The *B. burgdorferi* telomere resolvase, ResT, has been documented to be able to promote the fusion of hp telomeres in a reaction that is the chemical reversal of telomere resolution (29). ResT has also been shown to promote recombination between *rTels* to form HJs when telomere resolution is inhibited by the presence of negative supercoiling in the substrate DNA (30). Both of these reactions represent possible competing reactions that could promote genome instability if active *in vivo*. We assessed if wildtype TelA could promote these reactions and found that neither hp telomere fusion nor HJ formation is normally supported. However, deletion of the N-terminal domain allows HJ formation, especially with the hyperactivated TelA (107–442; D202A) mutant (Fig. 7). We also noted that hp telomere fusion becomes possible if ΔN mutants are supplemented with the N-terminal domain added *in trans* (Figs. 6 and S7). In both the telomere fusion and HJ formation reactions, a hyperactivated form of TelA and divalent metal ions is required. Besides being implicated in ssDNA annealing reactions, the N-terminal domain of TelA also appears to be involved in regulating the telomere resolution

activity of TelA to make it responsive to divalent metal ions and to suppress reversal and side reactions that could induce genome instability. Interpretation of the phenotype of N-terminal domain deletion alleles of TelA introduced *in vivo* to discover the biological role of ssDNA annealing will need to be interpreted with care due to the dual roles of the TelA N-terminal domain.

A possible role for the N-terminal domain in hp telomere capping

Aside from solving the end-replication problem, all telomeres must also solve the end-protection problem: how to avoid DNA ends from being degraded by nucleases or recognized as DNA damage. An understudied aspect of hp telomere biology is the mode of end protection employed in organisms with hp telomeres. This has best been studied in phage systems, typified by the N15 phage, that possess linear prophage genomes terminated by hp telomeres. The ΦKO2 telomere resolvase, TelK, has been reported not to turn over, leading to the suggestion that TelK may cap the resulting hp products (17). Additionally, in studies of an N15-derived linear cloning vector, it has been reported that prior expression of the N15 telomere resolvase, TelN, was required to protect hp ends of linear vector being transformed into *Escherichia coli* (34, 35). Finally, in a study that used the TelN reaction site *tos* integrated into the *E. coli* chromosome at the terminus, expression of TelN was necessary and sufficient for maintenance of the *E. coli* chromosome in a linear state (36). This implies that TelN is needed to create and cap the hp telomeres. A candidate region of TelA, should it also prove be involved in hp telomere capping, is the N-terminal domain that possesses ssDNA annealing activity. For ResT, we speculated that the annealing activity could play a role as a recombination mediator like RecOR since these genes are absent from the *B. burgdorferi* genome and ResT shares the property with RecOR of promoting annealing even with SSB-complexed ssDNA (21, 22). However, this hypothesis would seem to be untenable in *A. tumefaciens* since the standard RecOR mediator functions are encoded in the genome. If the ΔN TelA allele proves to be lethal *in vivo*, a defect in telomere capping would then be a strong candidate explanation.

Experimental procedures

DNAs

All oligonucleotides were purchased from Integrated DNA Technologies and are detailed in tabular form as Table S1 in the Supporting information. The pEKK392 plasmid substrate containing a 36-bp *rTel* used for telomere resolution reactions was generated by assembly of the *rTel* using oligonucleotides OGCB763/764 designed with 5′-GATC overhangs for cloning into BamHI-digested pUC19. The resulting plasmid was verified by DNA sequencing and named pEKK392. pEKK392 was linearized by SspI for use in plasmid telomere resolution assays.

Plasmid constructs for the expression of N-terminal His-tagged wildtype TelA, TelA (107–442), and TelA (1–106) proteins in *E. coli* were created as previously described in the study by McGrath *et al.* (23). The TelA (D202A), TelA (107–442; D202A), and TelA (R205A) mutants were generated through site-directed mutagenesis using the primer pairs OGCB772/773 and OGCB774/775, respectively, as detailed in Table S1. These plasmids were all verified through DNA sequencing, archived in DH5α, and transformed into Novagen's Rosetta(DE3)pLysS for expression and purification.

Proteins

The expression and purification of wildtype TelA, TelA (107–442), and TelA (1–106) were performed as previously described in the study by McGrath *et al.* (23). The TelA mutants D202A and R205A were expressed and purified as described for wildtype TelA. For expression of TelA (107–442; D202A), the culture was induced at 24 °C overnight with 0.25 mM isopropyl β-D-1-thiogalactopyranoside (IPTG). Lysate preparation and Ni-NTA affinity purification were performed as previously described for wildtype TelA (23). The heparin sepharose purification was performed in a similar manner as described for wildtype TelA with the following emendations. A 5-ml heparin sepharose column was used. The column was washed with ten column volumes of 0.25 M NaCl HG buffer (25 mM Hepes [pH 7.6], 0.2 mM EDTA, 10% (w/v) glycerol), followed by two column volumes of 0.35 M NaCl HG. The protein was eluted with one column volume of 0.5 M NaCl HG and collected in multiple fractions. Fractions were assayed for the presence of contaminating nuclease activity, and nuclease-free fractions were pooled. The protein prep concentrations were determined by BioRad's Bradford assay.

Telomere resolution assays

pEKK392 was linearized by SspI for use in telomere resolution assays. All plasmid telomere resolution assays were performed in buffer containing 25 mM Hepes (pH 7.6), 1 mM 1,4-dithiothreitol (DTT), 100 μg/ml bovine serum albumin, and 50 mM potassium glutamate. Reactions were supplemented with either EDTA or divalent metal ion as indicated in the relevant figure legends. The reactions were incubated at 30 °C. The conversion of 1.75 μg/ml of SspI-linearized pEKK 392 into two hp's was monitored with both timecourse and endpoint reactions. Timecourses were set up as 120 μl reactions, with 18-μl aliquots removed at the timepoints indicated in the figure legends and combined with SDS loading dye to a 1× final concentration (1× SDS load dye contains 20 mM EDTA, 3.2% [w/v] glycerol, 0.1% [w/v] SDS, and 0.0024% [w/v] bromophenol blue). Telomere resolution reactions were loaded to 0.8% (w/v) agarose/1× TAE gels and electrophoresed at 3 V/cm for 3 h and visualized by staining with 0.5 μg/ml ethidium bromide. Gel images were captured with a BioRad GelDoc system and quantified with QuantityOne software. Graphs and statistics were generated with Prism's GraphPad 6.0.

Half-site cleavage and hp telomere fusion assays

Half-site cleavage and hp telomere fusion reactions were performed in conditions optimized for telomere resolution using oligonucleotide substrates (25 mM Hepes [pH 7.6],

1 mM DTT, 2 mM $CaCl_2$, and 100 μg/ml bovine serum albumin). Protein (76 nM) (wt TelA, TelA (D202A), TelA (107–442), or TelA (107–442; D202A)), 380 nM of TelA (1–106), or some combination of the two proteins (TelA (107–442) + TelA (1–106), or TelA(107–442; D202A) + TelA (1–106)) was incubated with 5 nM of radiolabeled half-site or hp telomere (OGCB870*/871 and OGCB906*, respectively) and 35 nM of unlabeled substrate at either 30 °C for 30 min or 5 °C for 17 h. Reactions were halted by the addition of SDS load dye to a 1× final concentration prior to gel loading. All reactions were loaded to an 8% (v/v) PAGE/1× TAE/0.1% (w/v) SDS gel and electrophoresed at 13 V/cm for 105 min. Gels were subsequently dried and exposed to phosphor-imaging screens to be scanned with a phosphorimager. Control reactions were performed with a mock half-site cleavage or mock hp telomere (OGCB913*/914 and OGCB912*, respectively) that preserves the size and sequence composition of the telomere but scrambles the sequence into a nontelomeric sequence (Table S1).

HJ formation assays

All reactions were incubated in standard buffer conditions previously optimized for telomere resolution. Indicated proteins (76 nM) were combined with 10 μg/ml of pEKK392 and 70 nM of either oligonucleotide *rTel* (OGCB827*/828*) or mock *rTel* (OGCB855*/856*). The oligonucleotide *rTel* and mock *rTel* were partitioned between 20 nM of radiolabelled substrate and 50 nM of unlabeled substrate. Where indicated in the loading key to the figure, reactions were supplemented by addition 380 nM of the N-terminal domain (N). Control reactions omitted TelA addition. Reactions were incubated at 30 °C for 2 h followed by the addition of 5× SDS loading dye to a 1× final concentration prior to gel loading. For analysis of the resulting presumptive HJs, 10 μg/ml of pEKK392 was incubated with 40 nM of radiolabelled *rTel* (OGCB827*/828*) supplemented with 25 nM of unlabeled *rTel*, with or without 76 nM of TelA (107–442; D202A) at 30 °C for 2 h. Incubation was followed by buffer exchange with Illustra S-200 micro-spin columns. Fifty-microliter aliquots of the reaction were combined with CutSmart buffer and incubated with or without AhdI at 37 °C for 1 h. Reactions were subsequently divided into two aliquots and further incubated at 37 °C with or without T7 endonuclease I for 2 min. SDS loading dye (5×) was added to a 1× final concentration prior to gel loading. All reactions were loaded to a 0.8% (w/v) agarose 1× TAE gel and electrophoresed at 1 V/cm for 21 h. Gels were stained with 0.5 μg/ml ethidium bromide, imaged with a Biorad GelDoc system, and subsequently dried to Hybond N paper for exposure to phosphor-imaging screen.

Protein–protein cross-linking

Protein interactions between the N (TelA (1–106)) and C-terminal (TelA (107–442)) regions of TelA were probed through protein–protein cross-linking promoted by DSP. Wildtype TelA (240 nM), TelA (107–442) (240 nM), or 1 μM of TelA (1–106) were incubated in buffer containing 25 mM Hepes (pH 7.6), 55 mM potassium glutamate, 5 μg/ml of SspI-linearized pEKK392, and either 0.2 mM EDTA or 2 mM $CaCl_2$ to probe self-interactions. TelA (107–442) (240 nM) was incubated with 1 μM of TelA (1–106) to probe interactions between these separate domains. Additionally, the key role of the presence of DNA was verified by incubation of 240 nM of TelA (107–442) with1 μM of TelA (1–106) in 0.2 mM EDTA containing buffer with and without the added pEKK392 plasmid. All reactions were incubated at 30 °C for 10 min to allow protein–protein interactions to occur and then divided into two 80-μl aliquots: a sample without an added cross-linker and a sample with DSP added to a 40 μg/ml concentration. Further incubation at room temperature (RT) for 10 min was followed by quenching of excess DSP with Tris (pH 7.5) added to a final concentration of 50 mM. Incubation was then extended at RT for another 10 min. Protein loading dye (5×) without β-mercaptoethanol was added to the reactions to a 1× final concentration (1× final concentration contains 50 mM Tris [pH 6.8], 2% [w/v] SDS, 0.1% [w/v] bromophenol blue, and 10% [w/v] glycerol). Samples were loaded to a 16 × 16-cm 5%/10 to 18% (v/v) SDS-PAGE gradient gel for visualization with both Imperial Protein stain (Thermo Fisher) and α-His Western blotting.

Data availability

All data are contained within the manuscript and Supporting information.

Supporting information—This article contains supporting information (19).

Acknowledgments—We thank the virology and bacteriology research cluster for useful comments.

Author contributions—S. L. M. investigation; S. L. M. visualization; S. L. M. writing-original draft; S. H. H. project administration; S. H. H. resources; K. K. conceptualization; K. K. funding acquisition; K. K. supervision; K. K. writing-review and editing.

Funding and additional information—S. L. M. was supported by a University of Saskatchewan CoMRAD award. K. K. was supported by an NSERC Discovery Grant (RGPIN 04382-2017).

Conflict of interest—The authors declare that they have no conflicts of interest with the contents of this article.

Abbreviations—The abbreviations used are: DSP, dithiobis [succinimidylpropionate]; HJ, Holliday junction; hp, hairpin.

References

1. Olovnikov, A. M. (1973) A theory of marginotomy. The incomplete copying of template margin in enzymic synthesis of polynucleotides and biological significance of the phenomenon. *J. Theor. Biol.* **41**, 181–190
2. Ohki, R., Tsurimoto, T., and Ishikawa, F. (2001) *In vitro* reconstitution of the end replication problem. *Mol. Cell. Biol.* **21**, 5753–5766
3. Barbour, A. G., and Garon, C. F. (1987) Linear plasmids of the bacterium *Borrelia burgdorferi* have covalently closed ends. *Science* **237**, 409–411
4. Casjens, S., Murphy, M., DeLange, M., Sampson, L., van Vugt, R., and Huang, W. M. (1997) Telomeres of the linear chromosomes of Lyme

disease spirochaetes: Nucleotide sequence and possible exchange with linear plasmid telomeres. *Mol. Microbiol.* **26**, 581–596
5. Fraser, C. M., Casjens, S., Huang, W. M., Sutton, G. G., Clayton, R., Lathigra, R., White, O., Ketchum, K. A., Dodson, R., Hickey, E. K., Gwinn, M., Dougherty, B., Tomb, J. F., Fleischmann, R. D., Richardson, D., *et al.* (1997) Genomic sequence of a Lyme disease spirochaete, *Borrelia burgdorferi*. *Nature* **390**, 580–586
6. Rybchin, V. N., and Svarchevsky, A. N. (1999) The plasmid prophage N15: A linear DNA with covalently closed ends. *Mol. Microbiol.* **33**, 895–903
7. Goodner, B., Hinkle, G., Gattung, S., Miller, N., Blanchard, M., Qurollo, B., Goldman, B. S., Cao, Y., Askenazi, M., Halling, C., Mullin, L., Houmiel, K., Gordon, J., Vaudin, M., Iartchouk, O., *et al.* (2001) Genome sequence of the plant pathogen and biotechnology agent *Agrobacterium tumefaciens* C58. *Science* **294**, 2323–2328
8. Hertwig, S., Klein, I., Lurz, R., Lanka, E., and Appel, B. (2003) PY54, a linear plasmid prophage of *Yersinia enterocolitica* with covalently closed ends. *Mol. Microbiol.* **48**, 989–1003
9. Picardeau, M., Lobry, J. R., and Hinnebusch, B. J. (1999) Physical mapping of an origin of bidirectional replication at the centre of the *Borrelia burgdorferi* linear chromosome. *Mol. Microbiol.* **32**, 437–445
10. Ravin, N. V., Kuprianov, V. V., Gilcrease, E. B., and Casjens, S. R. (2003) Bidirectional replication from an internal ori site of the linear N15 plasmid prophage. *Nucleic Acids Res.* **31**, 6552–6560
11. Chaconas, G., Stewart, P. E., Tilly, K., Bono, J. L., and Rosa, P. (2001) Telomere resolution in the Lyme disease spirochete. *EMBO J.* **20**, 3229–3237
12. Bandy, N. J., Salman-Dilgimen, A., and Chaconas, G. (2014) Construction and characterization of a Borrelia burgdorferi strain with conditional expression of the essential telomere resolvase, ResT. *J. Bacteriol.* **196**, 2396–2404
13. Kobryn, K., and Chaconas, G. (2014) Hairpin telomere resolvases. *Microbiol. Spectr.* **2**. https://doi.org/10.1128/microbiolspec.MDNA3-0023-2014
14. Deneke, J., Ziegelin, G., Lurz, R., and Lanka, E. (2000) The protelomerase of temperate *Escherichia coli* phage N15 has cleaving-joining activity. *Proc. Natl. Acad. Sci. U. S. A.* **97**, 7721–7726
15. Kobryn, K., and Chaconas, G. (2002) ResT, a telomere resolvase encoded by the Lyme disease spirochete. *Mol. Cell* **9**, 195–201
16. Deneke, J., Burgin, A. B., Wilson, S. L., and Chaconas, G. (2004) Catalytic residues of the telomere resolvase ResT: A pattern similar to, but distinct from tyrosine recombinases and type IB topoisomerases. *J. Biol. Chem.* **279**, 53699–53706
17. Huang, W. M., Joss, L., Hsieh, T., and Casjens, S. (2004) Protelomerase uses a topoisomerase IB/Y-recombinase type mechanism to generate DNA hairpin ends. *J. Mol. Biol.* **337**, 77–92
18. Aihara, H., Huang, W. M., and Ellenberger, T. (2007) An interlocked dimer of the protelomerase TelK distorts DNA structure for the formation of hairpin telomeres. *Mol. Cell* **27**, 901–913
19. Shi, K., Huang, W. M., and Aihara, H. (2013) An enzyme-catalyzed multistep DNA refolding mechanism in hairpin telomere formation. *PLoS Biol.* **11**, e1001472
20. Mir, T., Huang, S. H., and Kobryn, K. (2013) The telomere resolvase of the Lyme disease spirochete, *Borrelia burgdorferi*, promotes DNA single-strand annealing and strand exchange. *Nucleic Acids Res.* **41**, 10438–10448
21. Huang, S. H., and Kobryn, K. (2016) The Borrelia burgdorferi telomere resolvase, ResT, anneals ssDNA complexed with its cognate ssDNA-binding protein. *Nucleic Acids Res.* **44**, 5288–5298
22. Huang, S. H., Hart, M. A., Wade, M., Cozart, M. R., McGrath, S. L., and Kobryn, K. (2017) Biochemical characterization of Borrelia burgdorferi's RecA protein. *PLoS One* **12**, e0187382
23. McGrath, S. L., Huang, S. H., and Kobryn, K. (2021) Single stranded DNA annealing is a conserved activity of telomere resolvases. *PLoS One* **16**, e0246212
24. Bankhead, T., and Chaconas, G. (2004) Mixing active site components: A recipe for the unique enzymatic activity of a telomere resolvase. *Proc. Natl. Acad. Sci. U. S. A.* **101**, 13768–13773
25. Tourand, Y., Lee, L., and Chaconas, G. (2007) Telomere resolution by *Borrelia burgdorferi* ResT through the collaborative efforts of tethered DNA binding domains. *Mol. Microbiol.* **64**, 580–590
26. Huang, W. M., DaGloria, J., Fox, H., Ruan, Q., Tillou, J., Shi, K., Aihara, H., Aron, J., and Casjens, S. (2012) Linear chromosome-generating system of *Agrobacterium tumefaciens* C58: Protelomerase generates and protects hairpin ends. *J. Biol. Chem.* **287**, 25551–25563
27. Lucyshyn, D., Huang, S. H., and Kobryn, K. (2015) Spring loading a pre-cleavage intermediate for hairpin telomere formation. *Nucleic Acids Res.* **43**, 6062–6074
28. Bankhead, T., Kobryn, K., and Chaconas, G. (2006) Unexpected twist: Harnessing the energy in positive supercoils to control telomere resolution. *Mol. Microbiol.* **62**, 895–905
29. Kobryn, K., and Chaconas, G. (2005) Fusion of hairpin telomeres by the *B. burgdorferi* telomere resolvase ResT: Implications for shaping a genome in flux. *Mol. Cell* **17**, 783–791
30. Kobryn, K., Briffotaux, J., and Karpov, V. (2009) Holliday junction formation by the *Borrelia burgdorferi* telomere resolvase, ResT: Implications for the origin of genome linearity. *Mol. Microbiol.* **71**, 1117–1130
31. Kashammer, L., Saathoff, J.-H., Lammens, K., Gut, F., Bartho, J., Alt, A., Kessler and, B., and Hopfner, K.-P. (2019) Mechanism of DNA end sensing and processing by the Mre11-Rad50 complex. *Mol. Cell* **76**, 382–394
32. Lu, C., Ward, A., Bettridge, J., Liu, Y., and Desiderio, S. (2015) An autoregulatory mechanism imposes allosteric control on the V(D)J recombinase by histone H3 methylation. *Cell Rep.* **10**, 29–38
33. Unnikrishnana, A., Amerob, C., Yadava, D., Stachowskia, K., Pottera, D., and Foster, M. (2020) DNA binding induces a cis-to-trans switch in Cre recombinase to enable intasome assembly. *Proc. Natl. Acad. Sci. U. S. A.* **117**, 24849–24858
34. Dorokhov, B. D., Strakhova, T. S., and Ravin, N. V. (2004) Expression regulation of the protelomerase gene of the bacteriophage N15. *Mol. Gen. Mikrobiol. Virusol.* **2**, 28–32
35. Godiska, R., Mead, D., Dhodda, V., Wu, C., Hochstein, R., Karsi, A., Usdin, K., Entezam, A., and Ravin, N. (2009) Linear plasmid vector for cloning of repetitive or unstable sequences in Escherichia coli. *Nucleic Acids Res.* **38**, e88
36. Cui, T., Moro-Oka, N., Ohsumi, K., Kodama, K., Ohshima, T., Ogasawara, N., Mori, H., Wanner, B., Niki, H., and Horiuchi, T. (2007) *Escherichia coli* with a linear genome. *EMBO Rep.* **8**, 181–187